Combustion, Explosion, and Shock Waves, Vol. 43, No. 1, pp. 104–113, 2007

Reflection of a Shock Wave in a Dusty Cloud

A. V. Fedorov,[1] Yu. V. Kharlamova,[1] and T. A. Khmel'[1]

UDC 532.529

Translated from *Fizika Goreniya i Vzryva*, Vol. 43, No. 1, pp. 121–131, January–February, 2007.
Original article submitted November 29, 2005.

The problem of shock-wave passage along a cloud of particles adjacent to a solid surface is studied numerically and analytically. The wave pattern of the flow near the shock wave reflected from this surface is analyzed within the framework of the equilibrium approximation of mechanics of heterogeneous media. The conditions of the transition from regular to irregular reflection from the substrate of the refracted shock wave inside the cloud are obtained analytically. The results of numerical simulations of a nonequilibrium flow in the two-velocity two-temperature approximation are compared with data obtained in the equilibrium approximation. Nonequilibrium and equilibrium flows are found to become more similar as the particle size decreases.

Key words: mechanics of heterogeneous media, shock waves, regular and irregular reflection, mathematical modeling.

INTRODUCTION

The study of interaction between a shock wave and a dusty layer is of interest both from the practical viewpoint of preventing industrial explosions and from the theoretical viewpoint in terms of studying the mechanisms of dust lifting and formation of dusty clouds.

A review of theoretical and experimental papers on mixing under a shock-wave action on dust-laden layers can be found in [1]; the review contains an analysis and formulations of the corresponding problems of mechanics of heterogeneous media. It should be noted here that many analytical and numerical studies were performed under the assumption that the particle size is rather small and the equilibrium approximation of mechanics of continuous media is valid. In this case, the motion of the surface layer of the suspension can be modeled by presenting it as a layer of a pseudo-gas of elevated density [2, 3]. In particular, the problem of passage of a shock wave (SW) along a layer of a coal-dust suspension in air was examined numerically in [2]. Replacement of the dusty layer by a similar layer of a cold gas allowed an analysis both within the framework of inviscid Euler equations and with allowance for viscosity and thermal conductivity (Navier–Stokes equations). The computation results revealed the internal system of waves in the layer, which was predicted in [4], and indicated that reflection of the refracted SW from the surface may be either regular or irregular. Occurrence of this or that type of reflection is associated in [2] with the influence of the dimensionless Atwood number characterizing the layer density and determining the angle of incidence of the SW refracted in this layer. SW interaction with a cloud of inert or reactive particles with a fixed mass fraction and different particle sizes was numerically simulated in [5] within the framework of the nonequilibrium approximation of mechanics of interpenetrating continua. The computations in a planar channel of a given width showed that the character of reflection is affected by the particle size, and the Mach stem height depends on the layer thickness.

Note that shock-wave processes in dusty media are significantly different from similar processes in gases, owing to nonequilibrium caused by momentum and energy exchange between the phases. Relaxation processes alter the qualitative wave pattern of the flow. For planar shock waves, for instance, this is manifested in nonmonotonic distributions of parameters behind the front in the downstream direction [6, 7]. The studies of SW propagation in a relaxing gas suspension and reflection of oblique shock waves on a wedge [8–11] revealed

[1]Khristianovich Institute of Theoretical and Applied Mechanics, Siberian Division, Russian Academy of Sciences, Novosibirsk 630090; fedorov@itam.nsc.ru.

0010-5082/07/4301-0104

some specific features; in particular, it was found [9] that changes in the particle size and the mass fraction of particles in the mixture may lead to generation of several principally different types of reflection. The relation between the critical angle of SW incidence and the Mach number is also more complicated than that in gaseous mixtures. Ben Dor et al. [9] studied the influence of particles on the criterion of the transition from regular to Mach reflection and found a linearly decreasing dependence of the critical angle of the wedge generatrix on the mass fraction of particles in the mixture for a prescribed Mach number. Saito et al. [11] analyzed the influence of nonequilibrium on the form of the curves of the transition from one type of reflection to the other. As the dependence of the angle of wave incidence on the distance covered by the SW along the wedge surface was found to be nonlinear, the transition curves were constructed in [11] as the wedge angle versus the Mach number of the frozen SW, as well as in the plane of the parameters "angle of the wedge generatrix–distance covered by the SW along the wedge." It follows from [9–11] that the transition curves for a dust-laden suspension and for a pure gas are principally different.

In the present work, we study the problem of propagation of a planar SW along a dust layer partly filling a planar channel. Here the SW is first refracted on the layer surface and then is reflected from the flat wall above which the cloud is located. The objective of the study is to clarify the influence of the dispersion (mass or volume fraction of particles and their size) on the wave pattern and SW reflection character.

The first part of the paper describes the derivation of transition criteria from regular to irregular SW reflection in a mixture of a gas and dust particles, similar to criteria available in gaseous media, in the equilibrium approximation (limiting case of a nonequilibrium flow) of mechanics of heterogeneous media. The effect of the volume fraction of particles on conditions of regular and Mach reflection of shock waves was observed (these parameters in gas mixtures are determined by the SW incidence angle and by the free-stream Mach number).

In the second part of the paper, the influence of the particle size (determining the processes of velocity and temperature nonequilibrium of the phases) and the layer thickness on the wave pattern, flow parameters, and type of reflection is quantified by means of numerical simulations of SW propagation along a dust-laden layer in a planar channel within the framework of equilibrium and nonequilibrium models of mechanics of heterogeneous media. The computed shock-wave structures are compared with appropriate flows described by analytical criteria of reflection in the equilibrium case.

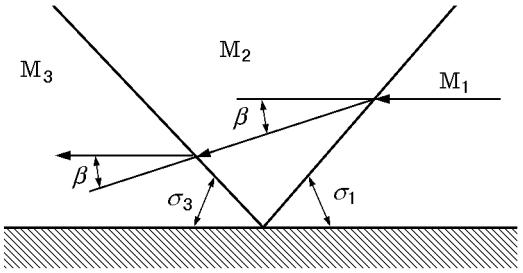

Fig. 1. Reflection of the shock wave from the wall.

1. EFFECT OF PARTICLES ON THE REFLECTION CRITERION FOR AN OBLIQUE SHOCK WAVE

We consider propagation of an oblique (refracted) SW along the wall in a mixture of a gas and fine dust particles. The states behind the SW front after its reflection are analyzed within the framework of the mathematical model of mechanics of heterogeneous media, which is equilibrium in terms of velocities and temperatures. The presence of particles is taken into account here by a modified equation of state.

The temperature, velocity, density, pressure, and internal energy of the equilibrium mixture are denoted by T, u, ρ, p, and e, respectively. The dimensionless mass fractions of the gas (subscript 1) and particles (subscript 2) are determined as $\xi_i = \rho_i/\rho$, where $\rho = \sum_i \rho_i$ and $\rho_i = \rho_{ii} m_i$ (ρ_i and ρ_{ii} are the mean and true densities of each phase, respectively), $\rho_{22} = \text{const}$, and m_i is the volume fraction of the ith phase. The heat capacities and the equilibrium ratio of specific heats of the mixture are expressed in a conventional manner: $c_p = \sum_i \xi_i c_{p,i}$, $c_v = \sum_i \xi_i c_{v,i}$, and $\gamma_e = c_p/c_v$. The equation of state with allowance for the volume fraction of particles is

$$p = \frac{\rho_1 RT}{1 - m_2} = \frac{\xi_1 RT}{w}, \qquad w = \frac{1}{\rho} - \frac{\xi_2}{\rho_{22}}, \qquad e = c_v T. \tag{1}$$

The equilibrium velocity of sound is presented as $c_e^2 = \gamma_e p/w\rho^2$.

The wave pattern of the examined flow in a coordinate system fitted to the shock-wave configuration is schematically shown in Fig. 1. The subscripts 1, 2, and 3 indicate the states ahead of the incident SW, behind the incident SW (but ahead of the reflected SW), and behind the reflected SW, respectively. The flow Mach numbers are determined as $\mathrm{M}_1 = u_1/c_{e1}$, where u_1 is the free-stream velocity (SW velocity in the laboratory

system), $M_2 = u_2/c_{e2}$, and $M_3 = u_3/c_{e3}$, where c_{ei} is the equilibrium velocity of sound in the corresponding domain. Let σ_1 be the angle between the wall and the front of the incident SW and σ_3 be the angle between the wall and the reflected SW. As the flow behind the reflected wave is assumed to be parallel to the wall, the angles of flow deflection β in states 2 and 3 are identical (see Fig. 1). To determine the parameters behind the incident and reflected shock waves, we use the known relations on an oblique shock wave:

$$\begin{gathered}
\rho_2 u_{2n} = \rho_1 u_{1n}, \quad p_2 + \rho_2 u_{2n}^2 = p_1 + \rho_1 u_{1n}^2, \\
u_{2\tau} = u_{1\tau}, \\
e_2 + \frac{p_2}{\rho_2} + \frac{u_{2n}^2}{2} = e_1 + \frac{p_1}{\rho_1} + \frac{u_{1n}^2}{2}, \\
\rho_2 u_{2n} = \rho_3 u_{3n}, \\
p_3 + \rho_3 u_{3n}^2 = p_2 + \rho_2 u_{2n}^2, \\
u_{3\tau} = u_{2\tau}, \\
e_3 + \frac{p_3}{\rho_3} + \frac{u_{3n}^2}{2} = e_2 + \frac{p_2}{\rho_2} + \frac{u_{2n}^2}{2}.
\end{gathered} \tag{2}$$

Here u_n and u_τ are the normal and tangential components of the velocity u determined by the formulas $u_{1n} = u_1 \sin\sigma_1$, $u_{1\tau} = u_1 \cos\sigma_1$, $u_{2n} = u_2 \sin(\sigma_1 - \beta)$, and $u_{2\tau} = u_2 \cos(\sigma_1 - \beta)$ for the incident SW and $u_{2n} = u_2 \sin(\sigma_3 + \beta)$, $u_{2\tau} = u_2 \cos(\sigma_3 + \beta)$, $u_{3n} = u_3 \sin\sigma_3$, and $u_{3\tau} = u_3 \cos\sigma_3$ for the reflected SW.

Applying some algebraic transformations, we obtain the following expressions for the angle of flow deflection β:

$$\tan\beta = \frac{\cot\sigma_1(\sin^2\sigma_1 - 1/M_1^2)}{(\gamma_e+1)/(2\rho_1 w_1) - (\sin^2\sigma_1 - 1/M_1^2)}, \tag{3}$$

$$\tan\beta = \frac{\cot(\sigma_3+\beta)(\sin^2(\sigma_3+\beta) - 1/M_2^2)}{(\gamma_e+1)/(2\rho_2 w_2) - (\sin^2(\sigma_3+\beta) - 1/M_2^2)}. \tag{4}$$

Note that Eqs. (3) and (4) in the approximation of a small volume fraction of solid particles in the mixture ($m_2 \approx 0$ and $\rho w \approx 1$) coincide with similar expressions for an ideal gas [12] with allowance for the ratio of specific heats dependent on the mass fraction of particles.

By consecutive transformations of Eqs. (2), we obtain the equations

$$\frac{1}{M_2^2} = \frac{w_1}{w_2 M_1^2}\frac{\sin^2(\sigma_1-\beta)}{\sin^2\sigma_1} \times \left(1 + \frac{\gamma_e}{\rho_1 w_1} M_1^2 \sin^2\sigma_1\right) - \frac{\gamma_e \sin^2(\sigma_1-\beta)}{\rho_2 w_2}, \tag{5}$$

$$\frac{1}{M_2^2} = \frac{w_3}{w_2 M_3^2}\frac{\sin^2(\sigma_3+\beta)}{\sin^2\sigma_3} \times \left(1 + \frac{\gamma_e}{\rho_3 w_3} M_3^2 \sin^2\sigma_3\right) - \frac{\gamma_e \sin^2(\sigma_3+\beta)}{\rho_2 w_2}, \tag{6}$$

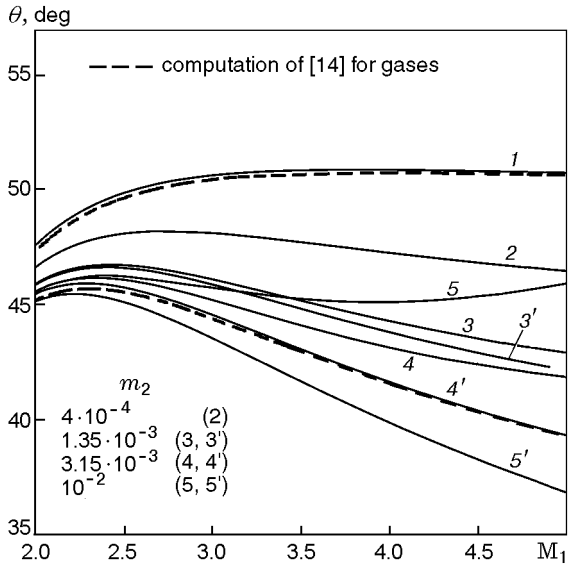

Fig. 2. Curves of the transition from regular to irregular reflection for a gas with $\gamma_1 = 1.4$ (1) and for various mixtures (2–5).

where

$$\rho_2 = \frac{\rho_1 \tan\sigma_1}{\tan(\sigma_1-\beta)}, \quad \rho_3 = \frac{\rho_2 \tan(\sigma_3+\beta)}{\tan\sigma_3}.$$

The total number of parameters in Eqs. (3)–(6) is six (M_1, M_2, M_3, σ_1, σ_3, and β). We are interested in the parameters M_1 and σ_1. To obtain a functional dependence between them (construct the transition curve), we use the von Neumann sonic criterion, which agrees well with experimental data for pseudosteady flows in gaseous media [13]:

$$M_3 = 1. \tag{7}$$

After eliminating M_2 and solving a quadratic equation with respect to $\cot\sigma_3$, we can use system (3)–(7) to determine the relation between σ_1 and M_1 in the form of a nonlinear equation, which is too cumbersome to be given here.

Figure 2 shows the computed dependences of the critical angle of the flow $\theta = 90 - \sigma_1$ (adjacent to the angle of the incident SW) on the SW intensity for several volume fractions of particles. These curves divide the domains of regular (above) and irregular (below) types of reflection. For $m_2 \approx 0$, the transition curve (solid curve 1) is rather close to the curve constructed on the basis of the data [14] for a gas with $\gamma_1 = 1.4$ (dashed curve 1), and the minor difference seems to be caused by the difference in transition criteria. (The transition to Mach reflection in [14] was associated with insolvability of the problem of determining the shock-wave configuration corresponding to regular reflection.) This fact

confirms that the mathematical models of the transition are similar [13].

The presence of particles in the mixture is manifested in a dual manner: in the change in the ratio of specific heats γ_e (effect of the loading ratio) and as a covolume in the equation of state (effect of the volume fraction). To estimate the effect of the latter factor in the transition from regular to Mach reflection, we performed computations with Eq. (1) replaced by the equation

$$p = \rho\xi_1 RT. \tag{8}$$

The corresponding results in Fig. 2 are marked by primed numbers. For comparatively small values of the volume fraction (up to $\approx 10^{-3}$), the data obtained with and without allowance for the parameter m_2 differ insignificantly (cf. curves 3 and 3′ in Fig. 2). An increase in the mass loading factor of the suspension ξ_2 reduces the value of the equilibrium ratio of specific heats γ_e, and the transition curve is shifted downward from the transition curve for $\gamma_e = 1.4$. The dependence $\theta(\mathrm{M}_1)$ is nonmonotonic is all cases, and there is a local maximum whose position depends on the mass fraction. The same behavior is observed by analyzing the data of [14] for gases. It is also worth noting that the results for the gas with the ratio of specific heats $\gamma_1 = 1.1$ [14] coincide with the computed curve 3′ [equation of state (8); $m_2 = 1.35 \cdot 10^{-3}$ and $\gamma_e = 1.1$]. Thus, the results for the mixture without allowance for the volume occupied by particles are consistent with available results on reflection of oblique shock waves in gases.

The effect of the volume occupied by particles becomes significant as the amount of particles in the mixture increases. For $m_2 = 3.15 \cdot 10^{-3}$ and 10^{-2}, a substantial difference is observed in results obtained with the use of Eq. (1) and Eq. (8) (cf. curves 4 and 4′, 5 and 5′ in Fig. 2). The behavior of the transition curves with allowance for the volume fraction of particles changes: in addition to a local maximum, there also appears a local minimum, after which the dependence $\theta(\mathrm{M}_1)$ starts increasing again. For $m_2 = 3.15 \cdot 10^{-3}$ (curve 4), the curve reaches an extreme value at $\mathrm{M}_1 \approx 5$. With increasing m_2, the position of the local minimum is shifted toward lower values of M_1 and approaches the local maximum (curve 5; $m_2 = 10^{-2}$). The value of the local maximum decreases, and the value of the local minimum increases. Thus, the curve tends to transform to a monotonically increasing dependence of the critical angle on the Mach number with a further increase in m_2. (Note that the volume fractions of the order of 0.1 for compression flows are outside the area of applicability of the present model.)

The dependence of the critical angle on the volume fraction of particles for fixed Mach numbers also

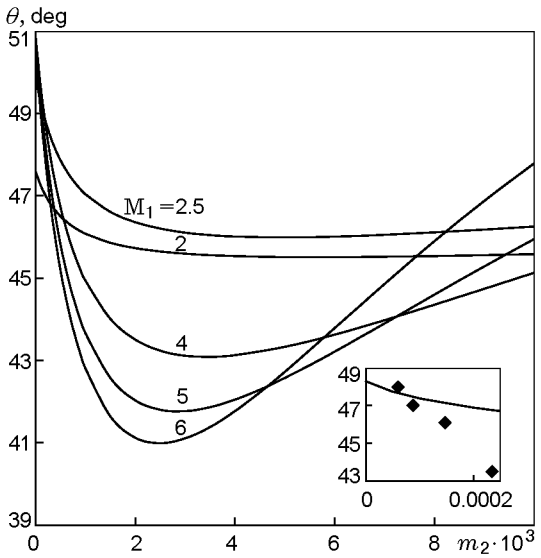

Fig. 3. Effect of the volume fraction on the transition angle for different values of the Mach number of the incident shock wave.

behaves in a complicated manner (Fig. 3). The initial values of the functions ($m_2 = 0$) here correspond to data for a pure gas. For moderate values of the SW amplitude, the values of θ decrease monotonically with increasing volume fraction. For low values of m_2, such a dependence qualitatively agrees with the numerical data of [9] (see the points in the insert in Fig. 3). The quantitative differences between the results of [9] and those in the present work and, correspondingly, results of [14] can be attributed to the fact that Ben Dor et al. [9] considered a slightly different problem: unsteady interaction of a planar SW with a wedge in a gas flow with heavier particles ($\rho_{22} = 4000\ \mathrm{kg/m^3}$, $m_2 \leqslant 2{\cdot}10^{-4}$, and $\mathrm{M}_0 = 1.5$).

As the Mach number increases, the dependence $\theta(m_2)$ becomes nonmonotonic, and the critical angle θ increases after a certain value of m_2 is reached (Fig. 3; $\mathrm{M}_1 = 4$). The greatest difference between the maximum and minimum values of the transition angle, caused by the effect of the volume fraction of particles, is observed for high Mach numbers.

The above-said implies that the types of SW reflection in suspensions of lighter and heavier particles with an identical mass fraction may be principally different. For $m_2 > 3 \cdot 10^{-3}$, the transition curve should be determined with allowance for the volume occupied by particles. A similar value in terms of the order of magnitude $m_2 \approx 10^{-2}$ was reported in [15] as the maximum admissible value at which the volume of particles in the analysis of equilibrium states of planar shock-wave structures can be neglected. Thus, the effect of

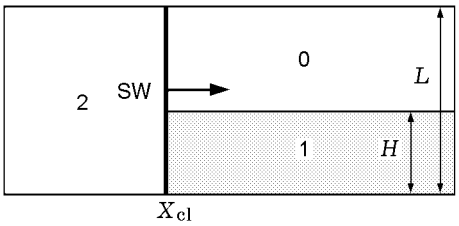

Fig. 4. Flow pattern: the domains show the initial conditions in the gas (0), the initial conditions in the mixture (1), and the conditions behind the SW in the gas (2).

particles on the shock-wave pattern and the transition from regular to irregular reflection occur not only owing to a change in the equilibrium ratio of specific heats but also owing to a change in the volume occupied by particles in the overall volume of the mixture.

2. EFFECT OF DISPERSION ON THE WAVE PATTERN OF THE FLOW AND THE CHARACTER OF SHOCK-WAVE REFLECTION IN A LAYER OF PARTICLES

We consider the problem of refraction and reflection of a planar SW in a layer of a gas suspension of fine solid particles within an identical fraction, which is also of independent interest because of the problems of "layered detonation" [5]. The shock-wave structure is assumed to occur in a semi-infinite rectangular cloud of the suspension, which is adjacent to the wall of a planar channel. The shock wave propagates over the channel from left to right over a quiescent gas without dust particles and interacts with the cloud of particles. The flow pattern is shown in Fig. 4.

To describe the SW interaction with the layer of particles suspended in the gas, we use two approaches of mechanics of heterogeneous media. In the first (equilibrium) approach, the mixture is computed as a one-velocity one-temperature continuum, as was done above. To describe the flow in this approximation, we use a system of conservation laws for a pseudo-gas, supplemented by the equation for the volume fraction of particles [2] and the equation of state in the form (1):

$$\frac{\partial \boldsymbol{Q}}{\partial t}+\frac{\partial \boldsymbol{F}}{\partial x}+\frac{\partial \boldsymbol{G}}{\partial y}=0,$$

$$\boldsymbol{Q}=\begin{pmatrix}\rho\\ \rho u\\ \rho v\\ \rho E\\ \rho m_2\end{pmatrix},\quad \boldsymbol{F}=\begin{pmatrix}\rho u\\ \rho u^2+p\\ \rho uv\\ (\rho E+p)u\\ \rho m_2 u\end{pmatrix},\quad \boldsymbol{G}=\begin{pmatrix}\rho v\\ \rho uv\\ \rho v^2+p\\ (\rho E+p)v\\ \rho m_2 v\end{pmatrix}.$$

Here $\boldsymbol{F}$ and $\boldsymbol{G}$ are the vectors of conservative fluxes in the corresponding directions; the parameters of the mixture are the density (ρ), the velocity components in the Cartesian coordinate system (u and v), the total energy (E), and the pressure (p).

In the second (nonequilibrium) approach of mechanics of heterogeneous media, the flow is described within the framework of a two-velocity two-temperature approximation. The equations of conservation of mass, momentum, and energy written for each phase and the closing relations are taken in the following form [5]:

$$\frac{\partial \rho_i}{\partial t}+\frac{\partial \rho_i u_i}{\partial x}+\frac{\partial \rho_i v_i}{\partial y}=0,$$

$$\frac{\partial \rho_i u_i}{\partial t}+\frac{\partial\,[\rho_i u_i^2+(2-i)p]}{\partial x}+\frac{\partial \rho_i u_i v_i}{\partial y}=(-1)^{i-1}(-f_x),$$

$$\frac{\partial \rho_i v_i}{\partial t}+\frac{\partial\,(\rho_i u_i v_i)}{\partial x}+\frac{\partial\,[\rho_i v_i^2+(2-i)p]}{\partial y}=(-1)^{i-1}(-f_y),$$

$$\frac{\partial \rho_i E_i}{\partial t}+\frac{\partial\,[\rho_i u_i(E_i+(2-i)p/\rho_1)]}{\partial x}+\frac{\partial\,[\rho_i v_i(E_i+(2-i)p/\rho_1)]}{\partial y}=(-1)^{i-1}(-q-f_x u_2-f_y v_2),$$

$$E_i=(u_i^2+v_i^2)/2+c_{v,i}T_i, \tag{9}$$

$$q=\frac{6m_2\lambda_1}{d^2}\,\mathrm{Nu}\,(T_1-T_2),$$

$$f=\frac{3m_2\rho_{11}}{4d}\,c_D|u_1-u_2|(u_1-u_2),$$

$$c_D(\mathrm{Re},\mathrm{M}_{12})=\Big(1+\exp\Big(-\frac{0.43}{\mathrm{M}_{12}^{4.67}}\Big)\Big)\times\Big(0.38+\frac{24}{\mathrm{Re}}+\frac{4}{\sqrt{\mathrm{Re}}}\Big),$$

$$\mathrm{Nu}=2+0.6\mathrm{Re}^{1/2}\mathrm{Pr}^{1/3},\ \mathrm{Re}=\rho_{11}d|u_1-u_2|/\mu,$$

$$\mathrm{M}_{12}=|u_1-u_2|\sqrt{\rho_{11}}\,/\sqrt{\gamma_1 p}.$$

The equation of state in such a flow of the suspension is used in the form (8), i.e., the volume fraction of particles is ignored.

In Eqs. (9), d is the particle diameter, c_D is the drag coefficient of particles, λ_1 is the thermal conductivity of the gas, Re, Nu, and Pr are the Reynolds, Nusselt, and Prandtl numbers, respectively, μ is the gas viscosity, and γ_1 is the ratio of specific heats.

The problem of SW interaction with a dust layer reduces to an initial-boundary problem with the following initial conditions:

$$t = 0: \quad \varphi = \begin{cases} \varphi_{\rm SW}(x), & 0 \leqslant x < X_{\rm cl}, \\ \varphi_{\rm cl}, & X_{\rm cl} \leqslant x < +\infty, \\ & 0 \leqslant y \leqslant h, \\ \varphi_0, & X_{\rm cl} \leqslant x < +\infty, \\ & h < y \leqslant L. \end{cases}$$

Here $\varphi = \{\rho, \rho u, \rho E, \rho m_2\}$ is the vector of the solution in the equilibrium approximation, $\varphi = \{\rho_1, \rho_2, \rho_1 u_1, \rho_2 u_2, \rho_1 E_1, \rho_2 E_2\}$ is the vector of the solution in the nonequilibrium approximation, $\varphi_{\rm SW}(x)$ are the parameters behind the SW front in the gas without particles, φ_0 is the initial state ahead of the SW front in the gas, $\varphi_{\rm cl}$ is the initial state of the mixture in the cloud, and $X_{\rm cl}$ determines the cloud boundary and the initial SW position. The initial values of gas and particle velocities ahead of the SW front and in the cloud have zero values. The particle density outside the cloud equals zero.

The following boundary conditions were used: a state corresponding to parameters behind the incident SW on the left boundary and conditions corresponding to $x = \infty$ on the right boundary (which was maintained on the right, at a certain distance from the transient SW).

The computations were performed for a mixture of particles of coal dust in air. The initial values of parameters were assumed to be $h = 20$ mm, $\rho_{11} = 1.177\,\text{kg/m}^3$ (air), $\rho_{22} = 1470\,\text{kg/m}^3$ (coal), $p_0 = 1$ atm, and $T_0 = 288$ K; the SW Mach number was M = 1.6.

To solve the initial-boundary problem in the equilibrium approximation, we used the CIP method proposed in [16] and adapted in [2] to problems of mechanics of equilibrium heterogeneous media. This method was successfully used to analyze flows with contact discontinuities [2]. The computations were performed on a uniform finite-difference grid with 1500×100 nodes. The problem in the nonequilibrium approximation was solved with the use of a total variation diminishing (TVD) scheme for the gas and the Gentry scheme for particles [17]. Such an approach was successfully tested on problems of heterogeneous detonation [5, 18]. When the problem was solved by this approach, the two-dimensional finite-difference grid was also uniform. The spatial step of the difference grid in both directions was 0.00025 m. The computational domain was expanded as the SW propagated further.

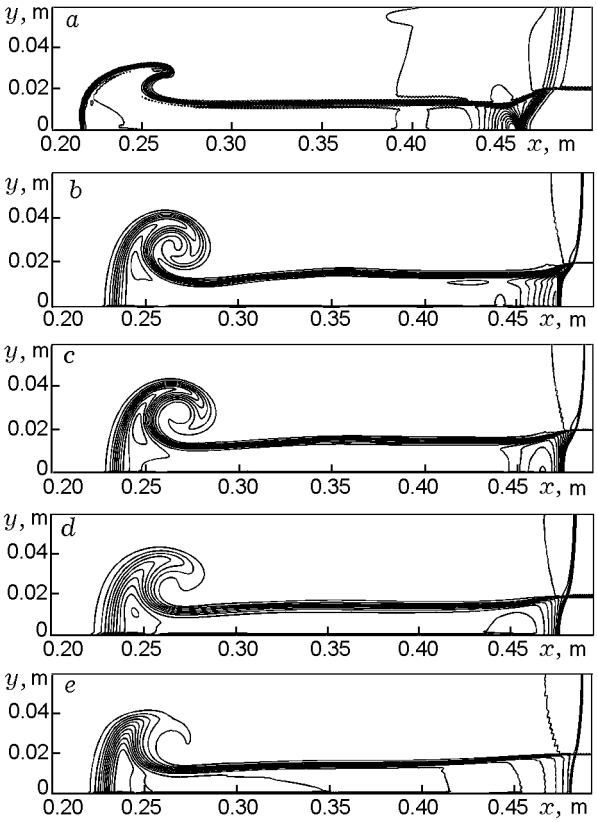

Fig. 5. Effect of the particle size on SW propagation along the suspension layer ($t = 0.9$ msec, $m_2 = 4 \cdot 10^{-4}$). Contours of equal density of the mixture for equilibrium approximation (a) and nonequilibrium approximation (b–e): $d = 0$ (a), 1 (b), 3 (c), 5 (d), and 10 μm (e).

In both methods, the computational error was less than 5% for all flow parameters.

The computed results are plotted in Figs. 5–9. Figure 5 shows a typical pattern of the flow, which is obtained by the nonequilibrium approximation of mechanics of heterogeneous media, in the form of density fields for the mixture at the time of 0.9 msec after SW interaction with the dust layer. Note that SW interaction with the cloud involves a certain period of flow unsteadiness, after which a pseudo-steady regime of SW propagation in the channel with SW refraction and reflection in the cloud of particles is established. As was shown above, within the equilibrium approximation, reflection can be either regular or irregular (with formation of the Mach stem). The wave pattern in the case of SW refraction and reflection in the layer is similar to

that considered in [2, 5]. The front of the leading SW experiences an inflection at the layer boundary. At the point of merging of the SW in the gas and the refracted SW in the layer, the contact (slip) surface separating the gas and the dust layer is also refracted. The layer behind the SW front is contracted, and its thickness becomes smaller than that ahead of the front. A certain increase in the layer thickness is reached when the SW reflected from the wall reaches the contact surface and interacts with the latter. In the flow illustrated in Fig. 5 (M = 1.6), this wave is weak and does not lead to any significant changes in the boundary, as was obtained in [5] for M = 3 and $d = 1$ μm. It is seen that the contact boundary between the gas and the mixture does not differ much from a horizontal line. Significant lifting of particles in Fig. 5 is observed only on the leading edge of the layer, where an unsteady vortex is formed owing to SW interaction with the rectangular edge of the cloud. A qualitative comparison of the data of numerical experiments performed within the framework of the equilibrium (Fig. 5a) and nonequilibrium (Figs. 5b–5e for particle size 1, 3, 5, and 10 μm, respectively) approximations shows that both approaches predict similar shapes of the cloud and vortex. A distinctive feature of the results obtained in the equilibrium approximation (Fig. 5a) by the CIP method [2, 16] is the clear-cut contact discontinuities at the cloud boundary and inside the cloud, but this technique does not allow accurate capturing of shock waves in the medium because the shock waves are smeared. In addition, it can be noted that the cloud contraction behind the leading SW in the equilibrium flow is more significant. Vice versa, the numerical calculations in the nonequilibrium approximation obtained by the TVD–Gentry scheme demonstrate some smearing of the contact and combined discontinuities in the mixture flow behind the SW in the layer. The latter is also caused by velocity and temperature relaxation processes, which is particularly noticeable as the particle diameter increases.

The pressure distributions on the channel wall behind the SW at the same time (0.9 msec) are plotted in Fig. 6. Note that the lengths of the relaxation zones are in nonlinear correlation with the particle size, because c_D and Nu depend nonlinearly on dimensionless flow parameters. For this reason, flows of gas suspensions, both in planar shock waves and in two-dimensional wave configurations, have different flow structures for different relations of relaxation parameters. As is seen from Fig. 6, the maximum pressure behind the Mach stem depends on the particle size. A drastic decrease in pressure after reaching the maximum in the equilibrium mixture is caused by the fact that a rarefaction wave formed owing to reflection of the SW

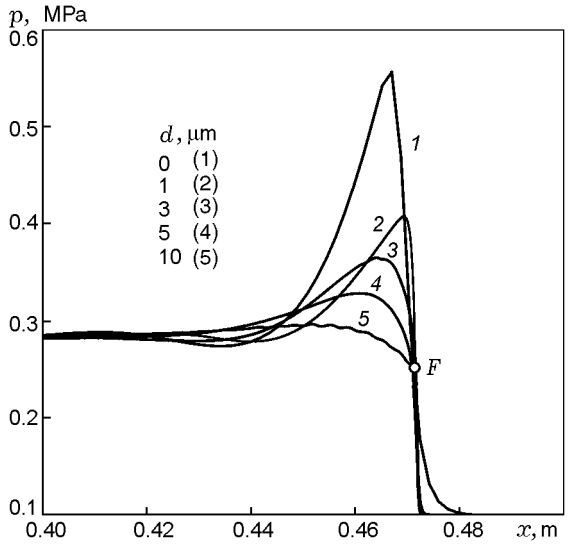

Fig. 6. Effect of the particle size on the pressure distribution on the wall: $t = 0.9$ msec; $m_2 = 4 \cdot 10^{-4}$; the data are obtained in the equilibrium approximation (1) and nonequilibrium approximation (2–5).

emanating from the triple point and refracted on the internal contact surface arrives on the wall [2]. In the gas–particle mixture, this wave interacts with the relaxation zone behind the Mach stem (whose length depends on the particle size: the greater the particle size, the greater the relaxation-zone length). Thus, the pressure maximum decreases with increasing particle size; for $d = 10$ μm, the pressure profile monotonically increases from a value at the front of the frozen shock wave (point F in Fig. 6) to the equilibrium value. Vice versa, as the particle size decreases, the pressure profile approaches the corresponding distribution obtained in the equilibrium model, i.e., generally speaking, there exists a limiting transition. Naturally, it is problematic to tell that such a transition definitely occurs.

To estimate the crossflow effects on the flow structure, computations were performed for different layer thicknesses normalized to the channel width. As the SW passes over the dust-laden cloud in the channel, the steady wave velocity is known to depend on the cloud width and mass fraction and to be independent of the particle size. Figure 7 shows the pressure distributions on the wall at one time instant. If the cloud occupies the entire width of the channel, the pressure first rapidly increases to the "frozen" value (pressure at the front of the frozen SW) and then continues to monotonically increase in the relaxation zone until it reaches the equilibrium value (curve 1 in Fig. 7).

In a layer of finite thickness, the pressure behind the Mach stem in the case of irregular reflection is higher

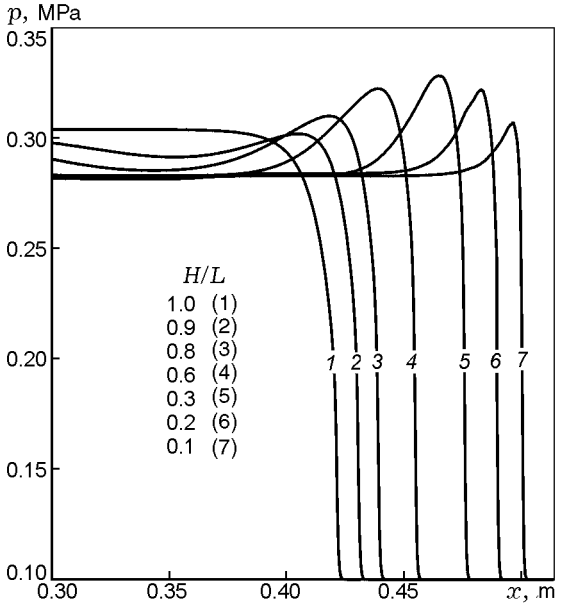

Fig. 7. Effect of the dimensionless layer thickness on the pressure distribution on the wall ($d = 5$ μm and $t = 0.9$ msec).

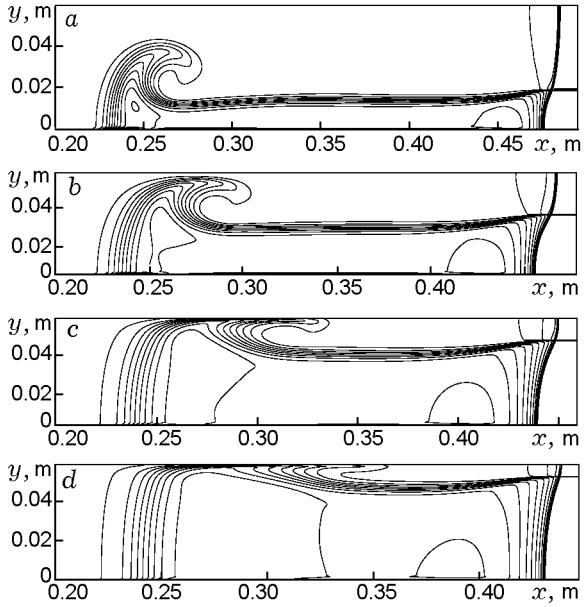

Fig. 8. Effect of the layer thickness on the wave pattern. Contours of equal density of the mixture: $d = 5$ μm, $m_2 = 4 \cdot 10^{-4}$, $t = 9 \cdot 10^{-4}$ sec, and $H/L = 0.3$ (a), 0.6 (b), 0.8 (c), and 0.9 (d).

than the equilibrium value. Therefore, the pressure distribution in the downstream direction is nonmonotonic: there is a pressure maximum behind the SW front, and then the pressure decreases to the equilibrium value. If the layer occupies more than half of the channel (curves 1–4 in Fig. 7), the crossflow effects are rather weak: the pressure peak is not very high. A further decrease in the layer thickness leads to a higher peak value, and the increase in pressure on the wall reaches the maximum value for a layer thickness equal to one third of the channel width (curve 5 in Fig. 7). After that, as is seen from Fig. 7 (curves 6 and 7), the effect of the decreasing dust-laden layer on the pressure on the wall becomes smaller. The maximum value of pressure decreases, and the relaxation zone also becomes smaller: it is limited by the crossflow size (thickness of the layer). The equilibrium value of pressure (in the far zone) corresponds now to the state behind the SW in the gas.

Thus, as the dimensionless thickness of the layer changes from $H/L = 1$ (the layer is completely filled by dust) to zero (pure gas in the channel), the peak pressure first increases and reaches a maximum and then gradually decreases and tends to the value behind the SW in the pure gas. Note that the particle size and, hence, the relaxation time remain unchanged in all computational events. Therefore, this behavior can only be caused by two following factors: a change in velocity of propagation of the shock-wave configuration (from the SW velocity in the mixture to the SW velocity in the pure gas) and relations between the geometric size of the layer and the length of the relaxation zones behind the SW. The SW velocities in the mixture and in the pure gas differ insignificantly, and the equilibrium states in Fig. 7 for $h = L$ and $h = 0.1L$ are also similar. Hence, the governing factor is the ratio between the scale of relaxation processes and the layer thickness.

Figure 8 shows the density fields of the mixture at the time $t = 0.9$ msec for different values of the layer thickness. For the minimum thickness of the layer (Fig. 8a, $H/L = 0.3$), the relaxation zone and the reflected wave approach the front of the leading SW and the wall to the maximum extent, which is manifested as closeness of the isochores to each other and to the frozen SW. Thus, the main changes in density of the mixture are observed in an immediate vicinity of the leading discontinuity. As the cloud width increases, this region becomes smeared, which is evidenced by greater gaps between the isochores. The flow in the cloud becomes closer to a one-dimensional flow, as the Mach stem increases. A comparison of the flows in Figs. 8b–8d shows that the type of SW reflection remains unchanged regardless of the layer thickness in this case, and the shapes of the incident waves are similar. Though the relaxation zones are commensurable with the layer thickness, the Mach stem is visible, which indicates that the reflection is irregular. It can be found, however, that

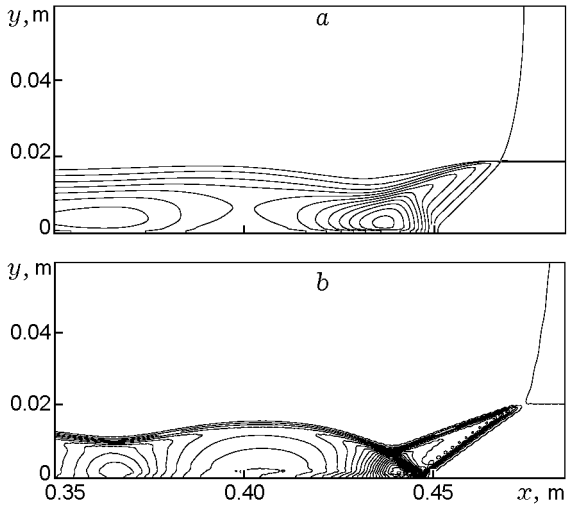

Fig. 9. Different types of reflection in a nonequilibrium gas suspension for $d = 3$ μm (a) and in the equilibrium approximation (b). Contours of equal density of the mixture ($m_2 = 10^{-3}$).

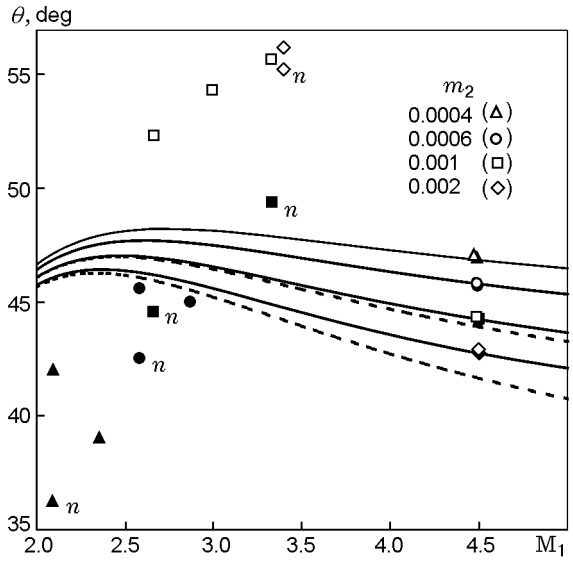

Fig. 10. Comparison of numerical data and analytical curves of the transition: the analytical curves are obtained with the use of the equation of state (8) (solid curves) and the equation of state (1) (dashed curves); the numerical data are plotted by open points (regular reflection), filled points (irregular reflection), and points marked by n (nonequilibrium approximation).

the angle of merging of the leading SW with the interface both in the gas and in the layer slightly changes with a change in the layer thickness. This means that the dimensionless thickness of the layer can affect the reflection type if the values of parameters are close to critical ones.

The effect of relaxation processes on the reflection type is illustrated in Fig. 9, which shows the wave patterns of the flow for M = 1.6 and $m_2 = 10^{-3}$ obtained in the nonequilibrium (Fig. 9a, particle size $d = 3$ μm) and equilibrium (Fig. 9b) approximations. Different types of reflection are obtained, depending on whether relaxation processes are taken into account or neglected. In the nonequilibrium mixture, the SW is reflected with a "smeared" Mach stem similar to [5] (because the relaxation-zone width is comparable with the channel width), whereas the reflection in the equilibrium mixture is regular.

The results of the numerical experiment were compared with analytical transition criteria derived in the first part of activities. Figure 10 shows the results of numerical computations for four values of the volume fraction of particles and the corresponding transition curves; for the volume fractions considered, these curves differ only slightly.

It is seen that the numerical results obtained in the equilibrium approximation are in good agreement with the transition curves (also determined for the equilibrium mixture) with appropriate ratios of specific heats.

The numerical results obtained in the nonequilibrium approximation (for the same Mach numbers and volume fractions) agree with the "equilibrium" curve only for M < 3, where the parameters of the nonequilibrium flow are little different from the equilibrium values. For M > 3, the numerical computations predict irregular reflection, whereas the equilibrium theory (and the equilibrium computations) predict regular reflection.

The results reported above testify that the relaxation processes have a significant effect on the character of SW reflection in a layer of a gas suspension.

CONCLUSIONS

Reflection of an oblique shock wave in a heterogeneous mixture of a gas and solid particles is examined in the paper numerically and analytically.

Curves of the transition from regular to irregular reflection in the mixture are obtained within the framework of the equilibrium approximation of mechanics of heterogeneous media in the plane "Mach number–angle of the incident shock wave." A significant effect of the volume occupied by particles on the critical transition angles for substantial concentrations of the solid component is established.

The influence of the particle size and dimensionless thickness of the layer on the wave pattern of the flow is numerically estimated within the framework of the two-

velocity two-temperature approximation of mechanics of heterogeneous media. The pattern of the mixture flow is demonstrated to become close to that obtained in the equilibrium approximation as the particle size decreases.

The data characterizing the reflection type, which were obtained numerically within the framework of the equilibrium model of mechanics of continuous media, are in satisfactory agreement with the transition criteria determined above.

The corresponding results for the nonequilibrium approximation are consistent with the equilibrium transition curves only for low Mach numbers and small particle sizes; for $M > 3$, the reflection types predicted by equilibrium and nonequilibrium computations are different, which is caused by the influence of relaxation processes on the character of reflection.

This work was supported by the Russian Foundation for Basic Research (Grant No. 03-01-00453).

REFERENCES

1. A. V. Fedorov, "Mixing in wave processes propagating in gas mixtures (Review)," *Combust., Expl., Shock Waves*, **40**, No. 1, 17–31 (2004).
2. A. V. Fedorov, N. N. Fedorova, I. A. Fedorchenko, and V. M. Fomin, "Mathematical simulation of dust lifting from the surface," *J. Appl. Mech. Tech. Phys.*, **43**, No. 6, 877–887 (2002).
3. D. Rayevsky and G. Ben-Dor, "Shock wave interaction with a thermal layer," *AIAA J.*, **30**, No. 4, 1135–1139 (1992).
4. A. A. Borisov, S. M. Kogarko, and A. V. Lyubimov, "Sliding of detonation and shock waves over liquid surfaces," *Combust., Expl., Shock Waves*, **1**, No. 4, 19–23 (1965).
5. T. A. Khmel' and A. V. Fedorov, "Interaction of a shock wave with a cloud of aluminum particles in a channel," *Combust., Expl., Shock Waves*, **38**, No. 2, 206–214 (2002).
6. G. F. Carrier, "Shock waves in a dusty gas," *J. Fluid Mech.*, No. 4, 376–382 (1958).
7. G. Rudinger, "Some properties of shock relaxation in gas flows carrying small particles," *Phys. Fluids*, **7**, No. 5, 658–663 (1964).
8. S.-W. Kim and K.-S. Chang, "Reflection of shock wave from a compression corner in a particle-laden gas region," *Shock Waves*, **1**, No. 1, 65–73 (1991).
9. G. Ben-Dor, O. Igra, and L. Wang, "Shock waves reflections in dust-gas suspensions," *Trans. ASME, J. Fluid Eng.*, **123**, 145–153 (2001).
10. O. Igra, G. Hub, J. Falcovitz, and B. Y. Wang, "Shock wave reflection from a wedge in a dusty gas," *Int. J. Multiphase Flow*, **30**, No. 9, 1139–1169 (2004).
11. T. Saito, M. Marumoto, and K. Takayama, "Numerical investigation of shock waves in gas-particle mixtures," *Shock Waves*, **13**, 299–322 (2003).
12. I. P. Ginzburg, *Aerogasdynamics* [in Russian], Vysshaya Shkola, Moscow (1966).
13. G. Ben-Dor, *Shock Wave Reflection Phenomena*, Springer-Verlag, New York (1992).
14. G. M. Arutyunyan and L. V. Karchevskii, *Reflected Shock Waves* [in Russian], Mashinostroenie, Moscow (1973).
15. G. Rudinger, "Relaxation in gas-particle flow," in: P. P. Wagner (ed.), *Nonequilibrium Flows*, Vol. 1, Part 1, Dekker, New York (1969), pp. 119–161.
16. T. Yabe, "A universal solver for hyperbolic equations for cubic-polynomial interpolation. 1. One-dimensional solver," *Comput. Phys. Comm.*, **66**, 219–232 (1991).
17. P. J. Roache, *Computational Fluid Mechanics*, Hermosa, Albuquerque (1976).
18. T. A. Khmel' and A. V. Fedorov, "Numerical simulation of detonation initiation with a shock wave entering a cloud of aluminum particles," *Combust., Expl., Shock Waves*, **38**, No. 1, 101–108 (2002).